Differential cross sections for incoherent scattering of γ rays by elements

Önder Şimşek
K. K. Education Faculty, Department of Physics, Atatürk University, 25240 Erzurum, Turkey
(Received 25 May 1999; revised manuscript received 27 July 1999; published 17 March 2000)

A method was developed for the accurate measurement of cross sections. This method involves the measurement of a differential incoherent cross section in terms of the *K*-shell cross section in the target, such that source strength, source-target, and target-detector solid angle terms cancel out in the final expression used to evaluate the differential incoherent scattering cross section. Differential cross sections for incoherent scattering of 59.54-keV γ rays by Zr, Nb, and Mo have been measured for angles ranging from 40° to 135° using a high-resolution Si(Li) detector. The experimental values have been compared with those estimated on the basis of the nonrelativistic Hartree-Fock wave functions.

PACS number(s): 32.80.Cy

I. INTRODUCTION

Incoherent scattering is an important mode of photon interaction with atoms in the energy range below 5 MeV. It changes the phase and usually the energy of the photon. The magnitude of changes depends on the scattering angle and the energy of the photon. The incoherent scattering by free electrons is Compton scattering and the bound electron counterpart is often called ''atomic Compton'' scattering. Over most of the region in which incoherent scattering is a major part of the total cross section, the Klein-Nishina theory is directly applicable [1]. Departures from the Klein-Nishina formula occur at low photon energies because of the electron binding effect. Many effects of the interaction of radiation with atoms depend on the so-called incoherent scattering function $S(x,Z)$ which is a measure of electron binding [2]. Values of $S(x,Z)$ have been calculated. Cromer and Mann [3] and Cromer [4] have evaluated the Waller-Hartree function $S(x,Z)$ using nonrelativistic Hartree-Fock atomic wave functions and these results have been tabulated by Hubbell *et al.* [5]. Most of the experimental work related to incoherent scattering is confined to higher photon energies [6–11]. Some authors have studied this process at lower energies [12–15]. The data will be very useful in calculating radiation attenuation, transport, and energy deposition in medical physics, reactor shielding, industrial radiography, and in a variety of other applications in addition to x-ray crystallography. Thus, there is a general need for subjecting the calculated values of incoherent scattering cross sections to extensive experimental tests.

With this in view, in the present work, we have measured total atomic incoherent scattering differential cross sections for Zr, Nb, and Mo elements at scattering angles from 40° to 135° by using a high-resolution Si(Li) detector.

II. EXPERIMENTAL METHOD

The experimental set up is shown in Fig. 1. The experiment was carried out using a filtered point source ^{241}Am (100 mCi) which emits monoenergetic (59.54-keV) γ rays. γ rays of 26.4 keV and *Np L* x rays coming from ^{241}Am are completely (~99.99%) filtered out with the help of graded filter of Pb, Cu, and Al of thickness 0.1, 0.1, and 1 mm, respectively, because even a small fraction of these radiations would produce sizable interference due to their large interaction cross sections with *K*-shell electrons. The graded filter consisting of Pb, Cu, and Al was used for preferential absorption of fluorescent x rays produced in the filter itself. Estimated transmission of 59.54-keV γ rays was ~45%. The γ source was placed in a lead collimator. γ rays of 59.54 keV from the ^{241}Am source are collimated on targets. The source with its collimator was rotated step by step with 5° annular increments about the horizontal axis. For the values 40°–135° of scattering angles, the spectra of scattered γ rays and emitted *K* x rays from the targets were recorded with a Si(LI) detector (full width at half maximum=160 eV at 5.96 keV, active area=12.5 mm^2, sensitive depth=3 mm) coupled to a 1024 computerized multichannel analyser through a spectroscopy automatic fine-tuning research amplifier. The amplifier shaping time constant that resulted in the best resolution was 6 μs and this value was used throughout the measurement. The built-in computer enabled data storage, peak resolution, background subtraction, and the determination of the net area of the *K* x-ray and incoherent scattered peaks. The spectra were analyzed using a quantitative x-ray analysis computer code Analysis of X-ray Spectra for Iterative Least-Squares Fitting (AXIL) [16–18]. The component of incoherent scattered photons in the spectrum is separated from the component of coherent scattered photons at small scattering angles using the AXIL x-ray analysis computer pro-

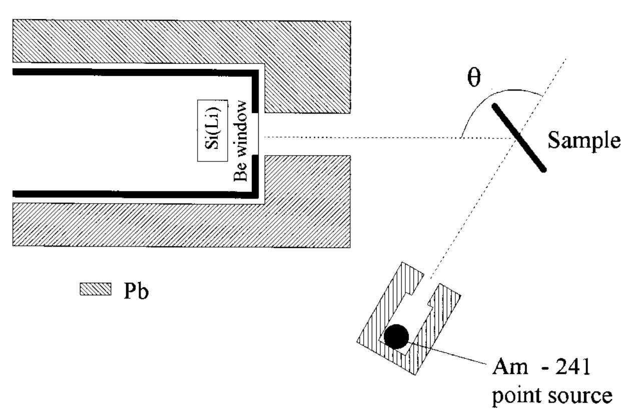

FIG. 1. Experimental setup.

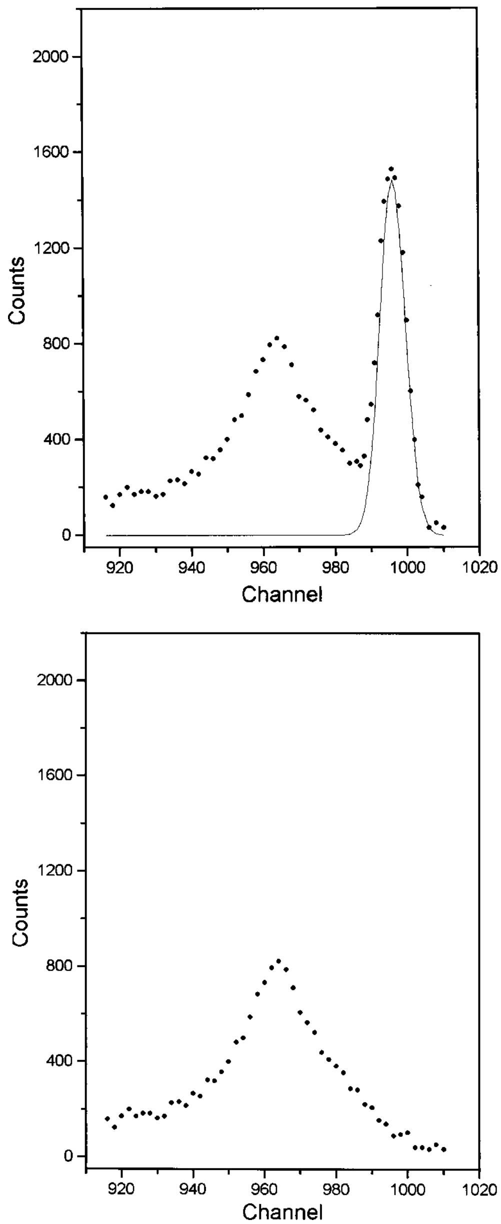

FIG. 2. (a) The net pulse-height spectrum of 59.54-keV photons scattered at 50° by Mo. The solid curve is a Gaussian for coherent peak. (b) Pulse-height data obtained after a subtraction of the elastic scattering contribution from the data displayed in (a).

gram. To obtain the net pulse-height spectra of scattered γ rays and emitted K x rays, a background spectrum without the target was subtracted from the spectrum acquired for the same time and experimental condition. The resulting pulse-height distribution of net scattered counts of Mo at 50° is displayed in Fig. 2(a). Elastic scattering peak was fitted as a Gaussian function. The solid curve in Fig. 2(a) represents Gaussian fitted elastic scattering peak. The elastic scattering contribution is obtained with the help of the solid curve. The elastic scattering contribution is subtracted from the data presented in Fig. 2(a) in order to determine the pulse-height distribution of Compton scattered γ rays. The resulting distribution is shown in Fig. 2(b).

The detector was shielded by a lead collimator so that only photons from a very small solid angle around the scattering foils could arrive at the detector. Thin elemental foils of Zr, Nb, and Mo were used as scatterers. The purity of foils was better than 99.9% and all the foils were of uniform thickness. The thickness of these foils ranged from 0.0129 to 0.0225 g/cm^2 for the elimination of multiple scattering and bremsstrahlung. The emitted K-shell x-ray counting rate and incoherent scattered radiation counting rate from the target of the element under study, as measured by the detector, are given by Eqs. (1) and (2), respectively [19]

$$N_{(K)}=I_o t \beta_{(K)} \sigma_{(K)} \frac{d\Omega}{4\pi} \varepsilon_{(K)} \omega_{(K)} \tag{1}$$

and

$$N_{(inc)}=I_o t \beta_{(inc)} \frac{d\sigma_{(inc)}}{d\Omega} d\Omega \, \varepsilon_{(inc)}, \tag{2}$$

where I_o is the incident beam intensity at the target, t is the sample mass per unit area in g/cm^2, $\beta_{(K)}$ and $\beta_{(inc)}$ are the absorption correction factors of the target, $\sigma_{(K)}$ is the K-shell photoelectric cross section of the element at the excitation energy of 59.54 keV, $\omega_{(K)}$ is the K-shell fluorescence yield, $d\Omega$ is the target-detector solid angle, $\varepsilon_{(K)}$ and $\varepsilon_{(inc)}$ are the detector efficiencies at the fluorescence x-ray and incoherent scattered γ-ray energies, $d\sigma_{(inc)}/d\Omega$ is the incoherent scattering differential cross section. From Eqs. (1) and (2),

$$\frac{d\sigma_{(inc)}}{d\Omega}=\frac{N_{(inc)}}{N_{(K)}} \frac{\beta_{(K)}}{\beta_{(inc)}} \frac{\varepsilon_{(K)}}{\varepsilon_{(inc)}} \frac{\sigma_{(K)}\omega_{(K)}}{4\pi}. \tag{3}$$

$N_{(K)}$ and $N_{(inc)}$ values are determined from the photopeak and incoherent scattered peak areas, $\sigma_{(K)}$ values were taken from a table [20], $\omega_{(K)}$ values were taken from the table of Hubbell *et al.* [21].

Since the emergent K x rays consist of two components, the procedure for calculation of $\beta_{(K)}$ described earlier is followed [22]. $\beta_{(K)}$ is computed from the relation

$$\beta_{(K)}=\frac{1-\exp\left[-\left(\frac{\mu_{(\gamma)}}{\cos\phi_1}+\frac{\mu_{(K)}}{\cos\phi_2}\right)t\right]}{\left(\frac{\mu_{(\gamma)}}{\cos\phi_1}+\frac{\mu_{(K)}}{\cos\phi_2}\right)t}, \tag{4}$$

where $\mu_{(\gamma)}$ and $\mu_{(K)}$ are the total attenuation coefficients [23] of the target at the energy of the incident γ rays and the weighted mean energy of the fluorescent K x rays, respectively.

The energies of the various peaks are taken to be the weighted mean energies of the various components incident under the corresponding peaks [24]. ϕ_1 and ϕ_2 are the angles of the incident and emitted photons with the target normal. For K x rays, Eq. (4) with $\mu_{(K)}$ at the weighted mean K x-ray energy can confidently be used [22].

The $\beta_{(inc)}$ value is similar to Eq. (4)

TABLE I. Comparison of experimental and theoretical incoherent scattering differential cross sections for Zr, Nb, and Mo in b/sr.

		$d\sigma/d\Omega$ (b/sr)					
		Zr		Nb		Mo	
θ (deg)	x (Å°)	Theor.	Expt.	Theor.	Expt.	Theor.	Expt.
40	1.644	1.823	1.846	1.861	1.805	1.896	1.965
45	1.840	1.771	1.815	1.805	1.768	1.839	1.918
50	2.032	1.698	1.730	1.731	1.671	1.748	1.713
55	2.220	1.604	1.652	1.636	1.590	1.652	1.607
60	2.404	1.501	1.520	1.532	1.574	1.563	1.547
65	2.583	1.420	1.505	1.452	1.510	1.482	1.541
70	2.758	1.337	1.403	1.365	1.392	1.381	1.427
75	2.927	1.282	1.230	1.310	1.375	1.324	1.392
80	3.090	1.224	1.170	1.250	1.275	1.277	1.324
85	3.248	1.198	1.152	1.224	1.248	1.242	1.272
90	3.400	1.170	1.134	1.197	1.185	1.209	1.260
95	3.545	1.178	1.208	1.205	1.230	1.233	1.244
100	3.683	1.184	1.243	1.211	1.250	1.238	1.305
105	3.814	1.227	1.280	1.255	1.310	1.289	1.356
110	3.938	1.269	1.304	1.299	1.340	1.328	1.380
115	4.055	1.311	1.405	1.341	1.360	1.372	1.427
120	4.164	1.390	1.473	1.422	1.450	1.454	1.510
125	4.264	1.430	1.520	1.464	1.537	1.497	1.567
130	4.357	1.509	1.570	1.544	1.574	1.579	1.602
135	4.442	1.587	1.618	1.624	1.591	1.661	1.696

$$\beta_{(inc)} = \frac{1-\exp\left[-\left(\frac{\mu_{(\gamma)}}{\cos\phi_1}+\frac{\mu_{(inc)}}{\cos\phi_2}\right)t\right]}{\left(\frac{\mu_{(\gamma)}}{\cos\phi_1}+\frac{\mu_{(inc)}}{\cos\phi_2}\right)t}, \tag{5}$$

where $\mu_{(\gamma)}$ and $\mu_{(inc)}$ are the total attenuation coefficients [23] at primary γ and incoherently scattered γ rays, respectively. The detector efficiency was measured using ^{241}Am, ^{133}Ba, and ^{54}Mn radioisotope testing sources according to an earlier method [25].

The theoretical incoherent scattering differential cross sections are calculated by using Eq. (6)

$$\frac{d\sigma_{(inc)}}{d\Omega} = \frac{d\sigma_{\mathrm{KN}}}{d\Omega} S(x,Z), \tag{6}$$

where $d\sigma_{\mathrm{KN}}/d\Omega$ is the Klein-Nishina cross section per electron, $S(x,Z)$ is the incoherent scattering factor, Z is the atomic number, $x=(\sin\theta/2)/\lambda$, θ is the angle of scattering, and $\lambda(A°)$ is the photon wavelength.

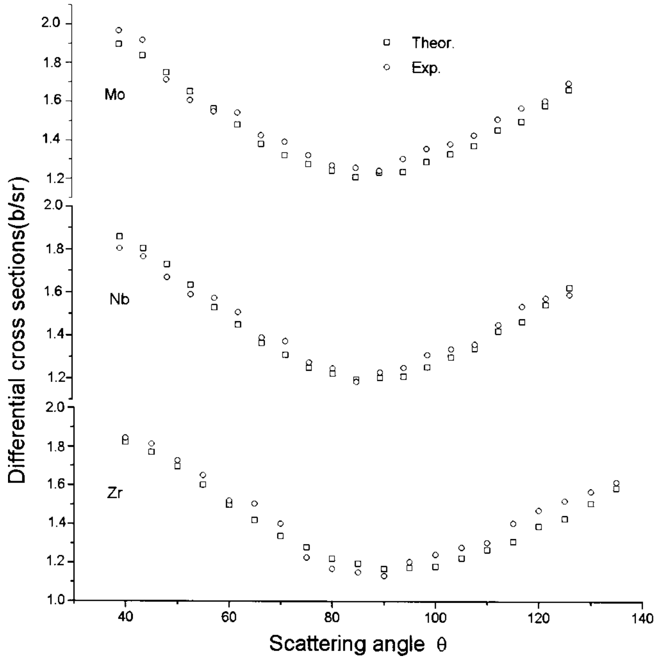

FIG. 3. Incoherent scattering differential cross sections as a function of scattering angle in b/sr.

III. RESULTS AND DISCUSSION

The present experimental results for incoherent scattering differential cross sections are listed with the theoretical values in Table I. In addition, the present experimental results are graphically compared with the theoretical results in Fig. 3. It can be seen from Table I and Fig. 3 that the present results are in good agreement with the theoretical results within the experimental errors. In order to reduce the statistical error the spectra have been recorded for a long time. The error associated in evaluating the photopeak area is 3%. The uncertainties in self-absorption correction factors were about 3%. The error in the detector efficiency is estimated to be about 3%. The overall error in the measured incoherent scattering differential cross sections is estimated to be less than 7%.

This present method is being used for the first time for the measurement of incoherent differential cross sections. In this method, the K x-ray counting rate [Eq. (1)] and scattering radiation counting rate [Eq. (2)] from target are measured at the scattering angles from 40° to 135°. From these equations, the incoherent differential cross section, $d\sigma_{(inc)}/d\Omega$, is obtained using Eq. (3). The use of Eq. (3) considerably simplifies experimental problems such as the estimation of source strength, source-target, and target-detector solid angles, etc.

[1] O. Klein and Y. Nishina, Z. Phys. **52**, 858 (1929).

[2] G. W. Grodstein, *X-ray Attenuation Coefficients from 10 keV to 100 MeV,* Natl. Bur. Stand. (U.S.) Circular No. 583 (U.S. GPO, Washington, DC, 1957).

[3] D. T. Cromer and J. B. Mann, J. Chem. Phys. **47**, 1892 (1967).

[4] D. T. Cromer, J. Chem. Phys. **50**, 4859 (1969).

[5] J. H. Hubbell, Wm. J. Veigele, E. A. Briggs, R. T. Brown, D. T. Cromer, and R. J. Howerton, J. Phys. Chem. Ref. Data **4**, 471 (1975).

[6] Saharsha M. Lad, G. Basavaraju, and P. P. Kane, Phys. Rev. A

42, 1267 (1990).
[7] J. C. Dow, J. P. Lestone, R. B. Taylor, and I. B. Whittingham, J. Phys. B **21**, 2425 (1988).
[8] P. P. Kane, J. Mahajani, G. Basavaraju, and A. K. Priyadarsini, Phys. Rev. A **28**, 1509 (1983).
[9] P. P. Kane, G. Basavaraju, and A. K. Priyadarsini, Nucl. Instrum. Methods **155**, 467 (1978).
[10] G. Pinto, N. G. Nayak, K. Siddappa, K. M. Balakrishna, and N. Lingappa, J. Phys. B **23**, 3759 (1990).
[11] S. G. Shivaramu and B. Sanjeevaiah, J. Phys. B **13**, 273 (1980).
[12] Y. Kurucu, S. Z. Erzenoğlu, R. Durak, and Y. Şahin, Appl. Spectrosc. Rev. **33**, 167 (1998).
[13] S. Z. Erzenoğlu, Y. Kurucu, and Y. Şahin, Phys. Scr. **57**, 503 (1998).
[14] D. V. Rao, R. Casereo, and G. E. Gigante, Phys. Scr. **50**, 314 (1994).
[15] D. V. Rao, R. Casereo, and G. E. Gigante, Can. J. Phys. **74**, 10 (1996).
[16] P. Van Espen, H. Nulles, and W. Maenhaut, in *Microbeam Analysis*, edited by D. E. Newburry (San Francisco Press, San Francisco, 1979), p. 265.
[17] P. Van Espen, H. Nulles, and F. Adams, Nucl. Instrum. Methods **142**, 243 (1977).
[18] P. Van Espen, H. Nulles, and F. Adams, Nucl. Instrum. Methods **145**, 579 (1977).
[19] Ö. Şimşek, Phys. Scr. **58**, 235 (1998).
[20] J. H. Scofield, Lawrence Livermore Laboratory (UCRL) Report No. 513626, 1973 (unpublished).
[21] J. H. Hubbell, P. N. Trehan, N. Singh, B. Chand, D. Mehta, M. L. Garg, R. R. Garg, S. Singh, and S. Puri, J. Phys. Chem. Ref. Data **23**, 339 (1994).
[22] S. K. Arora, K. L. Allawadhi, and B. S. Sood, J. Phys. B **14**, 1423 (1981).
[23] J. H. Hubbell, and S. M. Seltzer, Report No. NISTIR-5632, 1995 (unpublished).
[24] E. Storm, and I. Israel, Nucl. Data, Sect. A **7**, 565 (1970).
[25] D. D. Cohen, Nucl. Instrum. Methods **21**, 111 (1980).